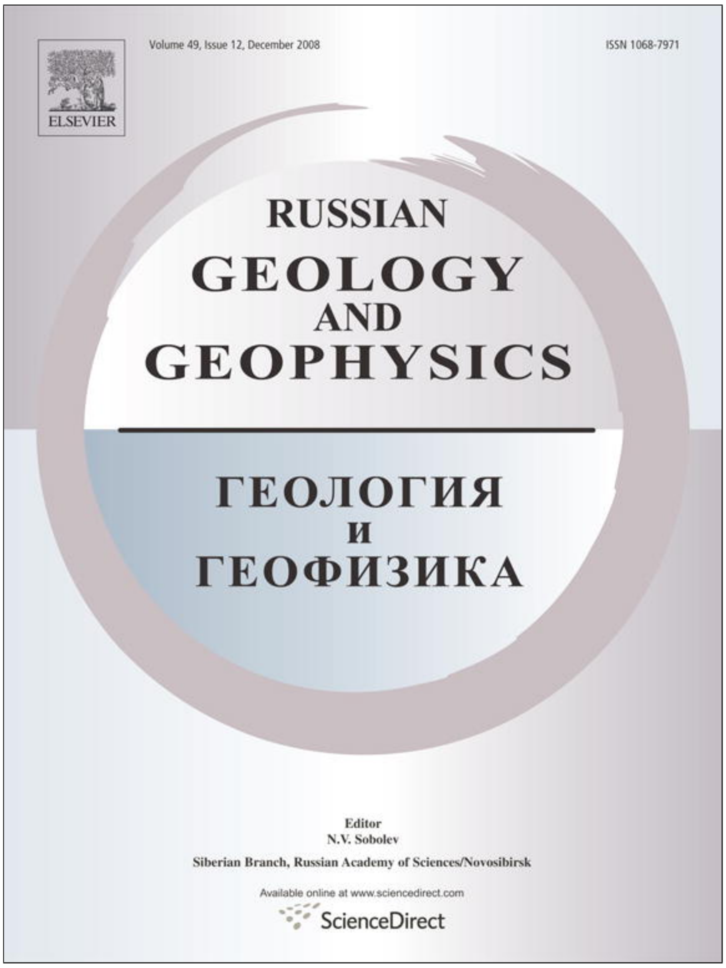
Volume 49, Issue 12, December 2008
ISSN 1068-7971
ELSEVIER
RUSSIAN
GEOLOGY
AND
GEOPHYSICS
ГЕОЛОГИЯ
и
ГЕОФИЗИКА
Editor
N.V. Sobolev
Siberian Branch, Russian Academy of Sciences/Novosibirsk
Available online at www.sciencedirect.com
ScienceDirect

Available online at www.sciencedirect.com
ScienceDirect
ELSEVIER
Russian Geology and Geophysics 49 (2008) 951–962
RUSSIAN GEOLOGY AND GEOPHYSICS
www.elsevier.com/locate/rgg

Quasi-periodic geomagnetic secular variation (from 1985–2005 world observatory data)

A.V. Ladynin * and A.A. Popova

Novosibirsk State University, 2 ul. Pirogova, Novosibirsk, 630090, Russia

Received 28 September 2007; accepted 21 April 2008

Abstract

We have discovered a 2–4 year periodicity in geomagnetic secular variation (SV) from data of 110 world magnetic observatories. The periodicity in the horizontal component (*H*) is most prominent and appears to be globally uniform in different regions, on all continents, and in both hemispheres. The quasi-periodic short-wavelength variations show up in the vertical component (*Z*) as well but locally superpose on long-wavelength regional anomalies. We presume that the short-period fluctuations may be produced by instability of the eccentric dipole (ED) axis proceeding from the analysis of the SV field and optimization modeling of the dipole field with varied ED parameters.

Keywords: Geomagnetic field; secular variation; quasi-periodic fluctuations; eccentric dipole; positions of dipole center and axial pole; dipole axis oscillations

Introduction

The patterns of secular variation (SV) of the Earth's main field have important implications for the internal sources of geomagnetism. There are various methods to study geomagnetic secular variation (Kalinin, 1984; Langel, 1987), such as (a) taking the difference between yearly spherical harmonic coefficients (g_m^n and h_m^n), including the time derivatives dg/dt and dh/dt in the analysis (Barraclough, 1976), or (b) analyzing observatory and repeat station survey data for the geomagnetic elements (*H*, *Z*, *D*, *I*, etc.) (Barraclough, 1976; Parkinson, 1983; Yanovskii, 1978). Comparison of observatory data and survey-data spherical harmonic models for successive years (Langel, 1987) at the observatory locations shows a significant inconsistency during different periods.

The SV studies using observatory and survey data imply comparison of isopor contour charts (differences of geomagnetic elements in 5-year epochs). Thus one can reveal SV "foci" (zones of equal annual changes contoured by isopors), their origin, drift, and breakup and divide the SV field into the drift and stable components. The method has certain limitations due to the uneven distribution of observatories and survey stations on the Earth's surface, but also has its advantages. Data from spatially fixed observatories and repeat stations are simpler to use because the differences in elements' values are free from the static field component, including magnetic anomalies produced by heterogeneity of the upper lithosphere.

Comparison of the spherical harmonic coefficients reveals time-dependent changes in the first harmonics which define the parameters of the geomagnetic dipole (its moment and eccentricity relative to the Earth's center). According to the spherical harmonic models, the dipole part of the main field is subject to regular changes, namely a decline of the dipole moment, a decrease in the angle of the dipole axis to the Earth's spin axis, a drift of the dipole away from the Earth's center, etc. (Ben'kova and Pushkov, 1980; Fraser-Smith, 1987; Dipole approximations..., 2003).

The dipole field makes about 90 % of the total geomagnetic field while its relative contribution to the SV field is much smaller than from the non-dipole part (Gauss, 1839; Langel, 1987; Parkinson, 1983; Yanovskii, 1978), which becomes obvious when comparing the changes in the first and higher-order harmonic coefficients (Langel, 1987). The charts of the main field components and their isopors synthesized from spherical harmonic coefficients for different years (www.bgs.ac.uk/images/charts/ipg) show a westerly drift of the geomagnetic elements, including the global magnetic anomalies. However, the spherical harmonic models miss the SV foci and their drift. To pick the latter, one needs the methods which, unlike SHA, do not smooth out the regional features of the SV field (Ben'kova et al., 1979).

* Corresponding author.
E-mail address: avlad@academ.org (A.V. Ladynin)

1068-7971/$ - see front matter
doi:10.1016/j.rgg.2008.04.006

The modern analytical models of the main field, such as IGRF or WMM, mostly employ satellite data which are complete and precise for the total intensity vector (*T*) only. Yet, the *T* measurements fail to account for exact changes in each component (*X*, *Y*, or *Z*), even if the input data for SHA include, as ties, SV estimates from several observatories (Dolginov et al., 1972; Ladynin et al., 2006a; Pushkov, 1972).

Having compared observatory and satellite estimates of geomagnetic secular variation, Barraclough (1985) found the former to be better for SV modeling. The reason is that the spherical harmonic analysis of satellite data introduces "orthogonal" errors of the non-dipole main field components (Backus, 1974; Lowes, 2000). The accuracy of SV estimates in spherical harmonic models is ±20 nT/yr, which is more than the real variations in many regions, including the SV foci. The SHA-derived estimates are put into IGRF models mostly for the main field interpolation but make a "very poor model" of the real geomagnetic variations (Lowes, 2003).

We (Ladynin et al., 2006a) discovered a 2–4 year periodicity in SV data from regional groups of observatories, which correlated among observatories within each group and region, and then studied them in more detail (Ladynin et al., 2006b). These quasi-periodic variations are missing from the IGRF models of the internal field. The difference between the SV estimates derived from observatory data and from IGRF models (Ladynin et al., 2006a,b) prompts that the causes of the short-period fluctuations may lie in the external field as well as in the changing parameters of the geomagnetic dipole. Below we discuss both hypotheses and estimate oscillations of the eccentric dipole (ED) axis which may be responsible for the observed SV periodicity.

The relationship of the 2–4 year quasi-periodic variations with the dipole field was recognized in observatory data from various regions of the world, all continents, and both hemispheres. To test the hypotheses, we modeled the components of the eccentric dipole field using the given coordinates of the dipole center and the direction of its axis corresponding to the position of the north ED axial pole. Thus we found the changes in the dipole parameters that fit the best the periodicity we discovered in the SV field.

Quasi-periodic geomagnetic fluctuations

We studied geomagnetic secular variations applying a differential approach. The changes were calculated for all geomagnetic elements at each observatory over a relatively short time span of 20 years, which allowed us to reliably identify the short-period fluctuations rather than taking them for noise as in (Langel, 1987; Wardinski, 2005; etc.).

The secular variations were calculated as differences of observatory annual means, from 110 world observatories for a period from 1985 to 2005 and three observatories for 100 years borrowed from www.geo-mag.bgs.ac.uk/cgi-bin/means. The observatory names are abbreviated according to the IAGA Observatory List.

We compared data averaged over regional observatory groups (four to seven observatories), then over continents, and finally over the two hemispheres. This multiple averaging provided removal of random features and regional SV trends and, on the other hand, made for the disparity in the number of observatories on different continents. Of 110 observatories, 37 are in Europe (5 regional groups), 25 in Asia (five groups), 22 in North America (four groups), 4 in North Africa, 4 in the Northern Pacific, and 18 in the whole southern hemisphere (four groups). Thus, 5/6 of observatories are in the northern hemisphere and only 1/6 are in the southern hemisphere.

Short-period fluctuations are the most prominent in the horizontal (*H*), inclination (*I*), and northward horizontal (*X*) components but are less stable in the components *Z* and *T* and almost absent from the declination (*D*) and eastward horizontal (*Y*) components. The discussion below is restricted to *H* and *Z* data (the time derivatives dH/dt and dZ/dt). The dH/dt and dZ/dt values are reported for a period of 1985 through 2005 as averaged over some regional observatory groups, all continents, and both hemispheres.

Figure 1 shows changes in the *H* and *Z* components from data of the central group of observatories in West Europe (WE-C). The dH/dt and dZ/dt plots share similarity in the presence of a 2–4 year periodicity, its distribution in the 20-year interval, and fluctuation amplitudes (~10–15 nT/yr) but have inverse peak-trough patterns. This group being located within a small area, significant difference in SV averages appears neither in *H* nor in *Z* components.

The setting is, however, different in large regions. See Fig. 2 for average *H* and *Z* variations in regional groups of European observatories. The *H* variations do not show much change but for the mean level. Note in this respect the observatories from western West Europe (WE-W), including Spain, UK, and France, where the average variations are higher than in other regional groups in *H* but lower in *Z*. The plots in Figs. 1 and 2 slightly differ in shape, possibly, because of the nonlinear trend in the group of central West Europe (WE-C), though the short-period fluctuations are similar.

The patterns from the Asian observatories are not so uniform. The dH/dt plot for Asia likewise has seven peaks as that for Europe, but with smaller amplitudes of annual means in the recent years. It is noteworthy that the quality of measurements reported from South Asia has worsened markedly for the past decade, especially the inclination and declination data, which is evident in the dZ/dt plot of Fig. 3. That is why we excluded the South Asian data from averaging over the Asian observatory groups and over the northern hemisphere.

The dZ/dt plots from Asia show a particular behavior. Earlier we discussed the special features of *Z* data from Japanese observatories (Ladynin et al., 2006a), which are obviously (Fig. 3) similar to those from most observatories in China and partly in Southeastern Asia. The dZ/dt changes have smaller amplitudes than the regional-scale long-wavelength fluctuations for different regions. Note that the trends from all regions show a sign reversal in 1995–1997. We cite no data

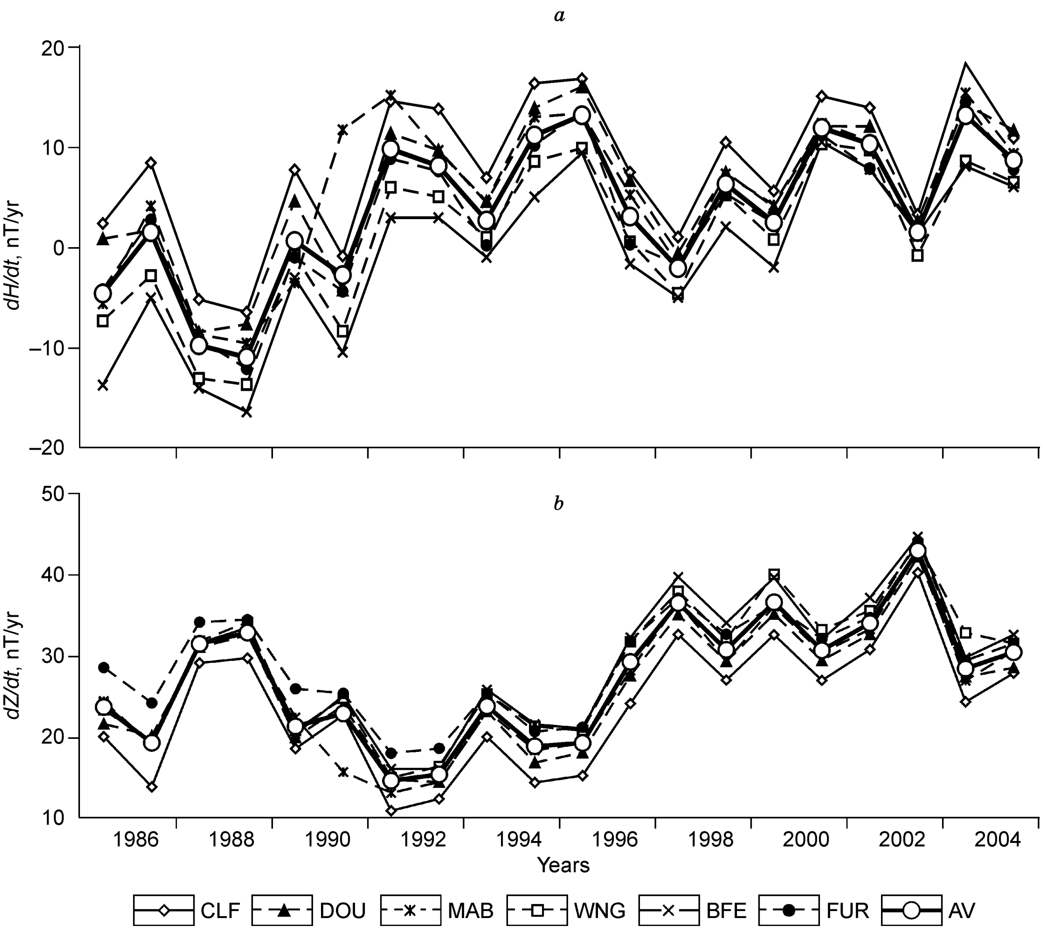

Fig. 1. Variations of *H* (*a*) and *Z* (*b*) at observatories in West Europe (center). CLF, DOU, MAB, WNG, BFE, and FUR are observatories. AV stands for averaged.

for the other continents of the northern hemisphere as they do not differ much from the European data.

Figure 4 shows SV in the *H* and *Z* components averaged over the continents and over the whole northern hemisphere. The hemisphere-average *dZ*/*dt* are given in two scales: in the same scale as for all plots and in a larger scale in order to highlight the quasi-periodic fluctuations against large regional-scale changes in different continents.

Thus, the fluctuations in the *H* and *Z* components mostly have similar amplitudes and opposite phases in groups of observatories as well as in the averages over groups and continents and over the northern hemisphere. Their amplitudes remain almost the same after multiple averaging, i.e., random effects cause no significant influence on the final estimates.

The plots from Asia and North Africa occupy extreme positions in both panels (*a* and *b* in Fig. 4). The *dH*/*dt* changes are generally similar for Europe, North America, and the northern Pacific while the *dZ*/*dt* plot for Europe is notably above those for North America and the Pacific. The mean levels of the *dH*/*dt* plots differ for less than 35 nT/year, whereas the difference in *dZ*/*dt* reaches 80 nT/year. The extreme values of *dH*/*dt* and *dZ*/*dt* are related in approximately the same way: the regional trends in *dZ*/*dt* have amplitudes twice as large as in *dH*/*dt*.

See a marked regional trend in Asian data in Fig. 4, *b*, which we mentioned above. The quasi-periodic fluctuations in the hemisphere-average *dZ*/*dt* plot being poorly discernible on the background of a large difference between the respective plots averaged over Asia and Africa, we had to reproduce it in a larger scale.

The plots in Fig. 5 are the changes *dH*/*dt* and *dZ*/*dt* in regions of the southern hemisphere and the hemisphere average, compared with the average over the northern hemisphere. The *dH*/*dt* plot for the southern hemisphere is 20 nT/yr lower than the respective plot from the northern hemisphere, because of data from South America. The *dZ*/*dt* levels are similar in South Africa, Australia, and in the Indian ocean because of their regional trends which are more significant than the trends of *dH*/*dt*.

The patterns in the *H* and *Z* components are obviously regular. The 2–4 year periodicity is especially prominent in the horizontal component *H* being synchronous in data from all observatories and in the averages over observatory groups and continents. The *Z* fluctuations in data from Japan, China, and Southeastern Asia are less regular. The 20-year span includes seven peaks and six troughs in the *H* plot while the pattern for *Z* with six peaks and seven troughs is generally less distinct except for few local areas.

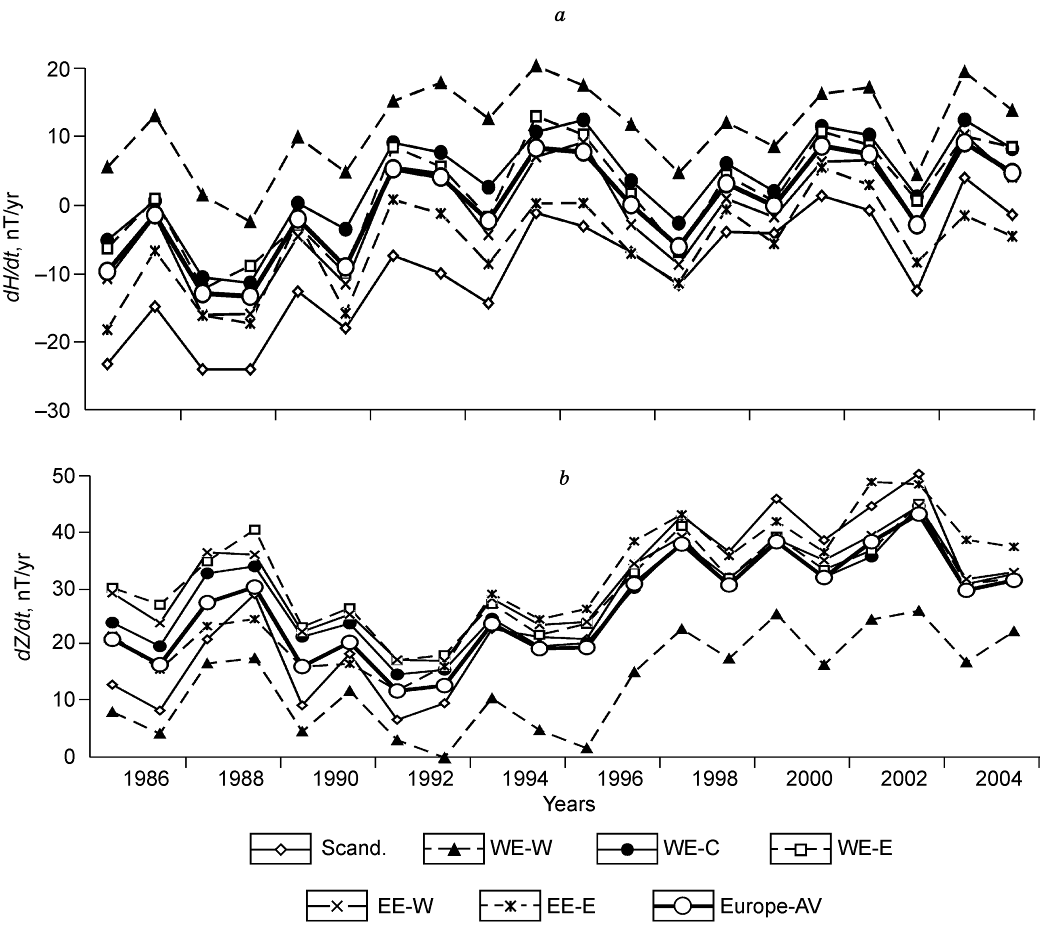

Fig. 2. Variations of H (*a*) and Z (*b*) averaged over groups of observatories in Europe. Groups of observatories are abbreviated as: Scand — Scandinavia, WE-W — West Europe-west, WE-C — West Europe-center, WE-E — West Europe-east, EE-W — East Europe-west, EE-E — East Europe-east, Europe-AV — Europe average.

The global-scale similarity of the quasi-periodic (period 2–4 years) SV patterns of H and Z may be due to changes either in the external ionospheric-magnetospheric field or in the parameters of the dipole responsible for the main part of the internal field.

The SV field, especially its Z component, depends largely on long-wavelength regional trends with periods from 5 to 30 years, which are most often attributed to convective flow on the core surface (Huy et al, 1998; Langel, 1987; Wardinski, 2005) rather than to dipole variations. To check the dependence of the short-period fluctuations on the eccentric dipole parameters, we excluded the 5-30 year trends in the form of the second-degree polynomial. See Fig. 6 for the behavior of dH/dt and dZ/dt and their time dependence with removed long-period trends for the northern and southern hemispheres and for two most distantly spaced observatories (HAD in Europe, UK, and EYR in Australia).

We tested the SV estimates for H and Z in long (100 years) series of data from three observatories (VAL in Ireland, API in the Pacific ocean, and ABG in India) and found the same periodicity as in the 20-year series of observatory data (see H variations in Fig. 7).

The number of extremes in the 100-year dH/dt series from the three observatories corresponds to an average period of 3.3 years. The peaks are unevenly distributed, with six or seven peaks in each 20-year interval for each observatory, spaced at 2 to 4 years, as well as in the 20-year series from 110 observatories. The short-period fluctuations are superposed on a longer-wavelength periodicity of 20–70 years, specific to different observatories. Note that the 2–4 year quasi-periodic fluctuations look like noise in the long series (Fig. 7) and would be hard to pick without a priori knowledge of results for the 20-year series. That may be the reason why this periodicity was never reported before in publications on geomagnetic secular variation.

We came to recognize the quasi-periodic fluctuations using the differential approach with the main focus on dH/dt, dZ/dt, etc., over short time intervals of 20 years, recorded at small regional groups of observatories. The differential approach is not new. For instance, Wardinski (2005) applied it to analyze 1980–2000 data from many observatories to model core surface flow as a cause of jerks and obtained variations with decadal and longer periods. He reported no three-year periodicity, however, possibly because he took it for noise.

Thus, the 2–4 year periodicity of secular variation is prominent in the H component (also in I and X), is present though slightly less stable in Z (and T), but never found in D and Y.

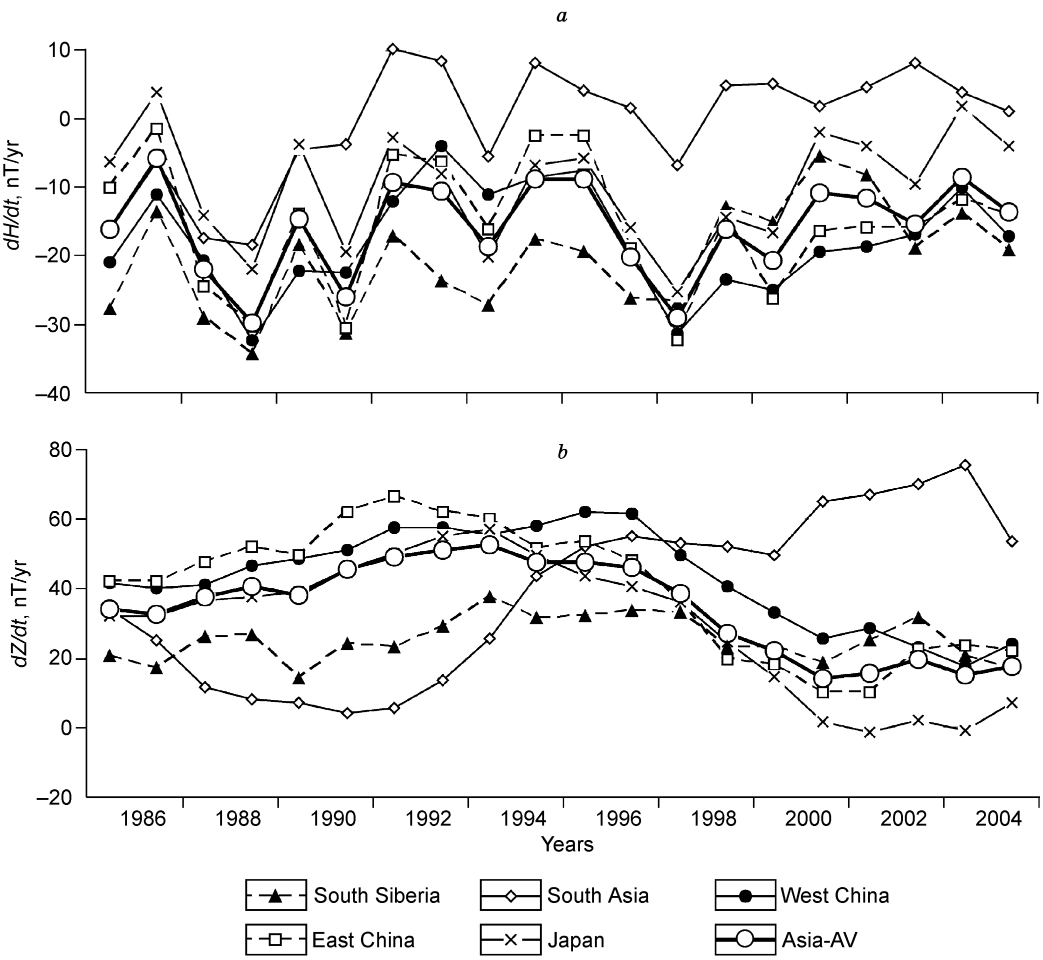

Fig. 3. Variations of *H* (*a*) and *Z* (*b*) averaged over groups of observatories in Asia and over Asian continent.

There naturally arises the question of its origin. This periodicity may result from time-dependent changes in current systems which generate the main field (in the ionosphere or in the outer core). The ionospheric current systems are controlled by solar-terrestrial links. Relevant data on quasi-biannual oscillations in some solar activity parameters can be found in (Ivanov-Kholodnyi et al., 2002) and temperature variations at different atmospheric heights are reported in (Fadel et al., 2002), over observation periods of 19 and 7 years, respectively. The cycles revealed in the cited papers slightly exceed 2 years on average, i.e., they are 1.5 times shorter than the periodicity we discovered but approach a harmonic solar cycle of 2.4 years (894 days) according to Wardinski (2005). The instability of the short SV periods, unlike the stable solar cycles, is another reason why we doubt about their linkage with solar or atmospheric processes. On the other hand, the causes of quasi-biannual periodicity in solar activity and upper atmospheric temperatures have never been proved to lie with changes in the external geomagnetic field. This relationship requires a special study which is beyond our competence.

We suggest that the short-wavelength periodicity in global SV patterns results from variations in the dipole field, the main field without global magnetic anomalies. To check this hypothesis, we analyzed the geomagnetic elements in eccentric dipole models with varied parameters. This modeling became possible when the appropriate equations were obtained (Ladynin, 2008), which are used below.

Changes in the eccentric dipole parameters according to quasi-periodic SV fluctuations

Changes in five parameters of the eccentric dipole (ED) are impossible to determine unambiguously from the *dH*/*dt* and *dZ*/*dt* functions without additional information or some constraints. Increasing data collections cannot make the estimates more reliable because the 2-4 year SV cycles of *H* and *Z* are almost identical globally.

Important are the phases and the amplitudes of the fluctuations. One can obtain phase-amplitude relationships of changes in the ED field components associated with changes in the ED parameters (coordinates of the dipole center and direction of its moment, i.e., the north axial pole position) in models where the latter parameters are user-specified. Then, having compared the observed and computed phases and amplitudes, one can select the ED parameters that are most likely responsible for the 2–4 year SV periodicity. The final

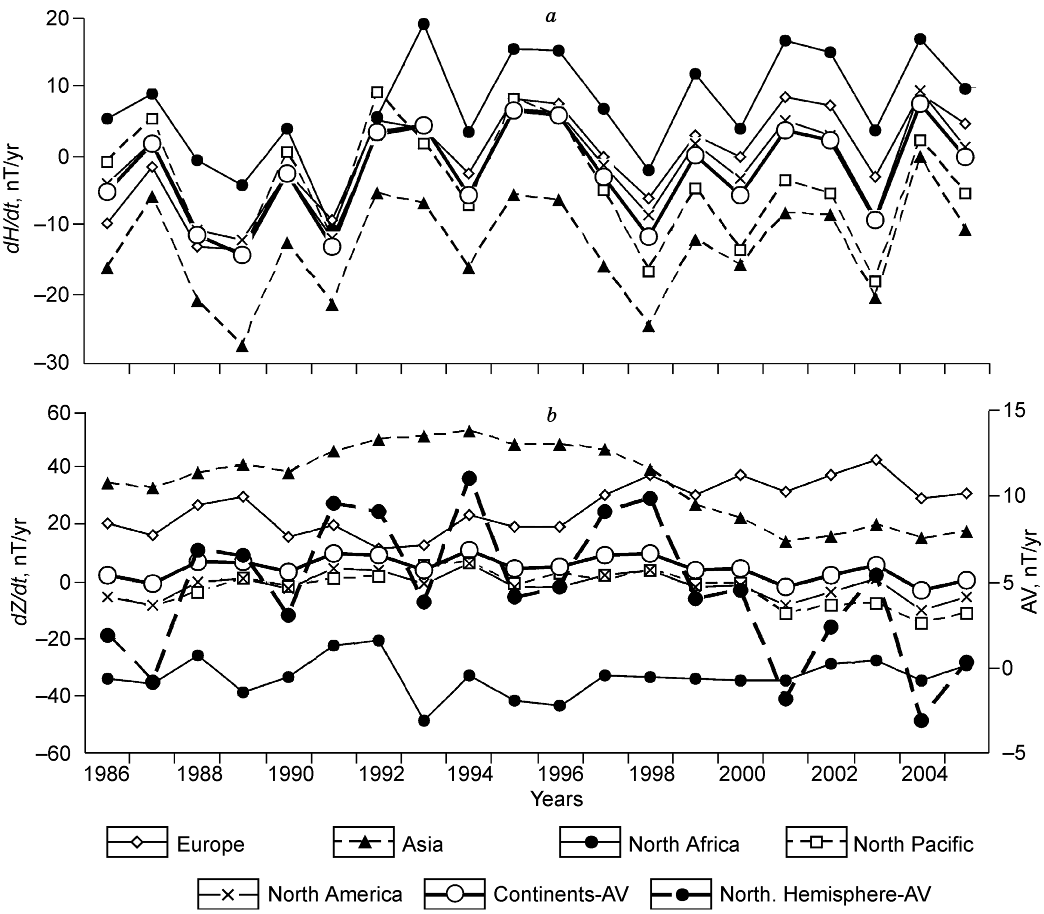

Fig. 4. Variations of *H* (*a*) and *Z* (*b*) averaged over continents and over whole northern hemisphere.

step of modeling consists in optimization fitting of the changes in the ED parameters to the observed *H* and *Z* patterns of secular variation. The *X*, *Y*, *Z* components of the ED field at an arbitrary point *A* (θ, λ) in the Cartesian coordinates (origin at an observation point on the Earth's surface, northward *x* axis, eastward *y* axis, and downward *z* axis) are expressed via the total intensity components X_c, Y_c, Z_c in the Cartesian coordinates (origin at the Earth's center, z_c axis along the Earth's spin axis, x_c axis along the Greenwich meridian, and eastward y_c axis) and are found as

$$X = X_c \cos\theta \cos\lambda + Y_c \cos\theta \sin\lambda - Z_c \sin\theta;$$

$$Y = -X_c \sin\theta \sin\lambda + Y_c \sin\theta \cos\lambda;$$

$$Z = X_c \sin\theta \cos\lambda + Y_c \sin\theta \sin\lambda + Z_c \cos\theta. \quad (1)$$

The X_c, Y_c, Z_c components of the total intensity vector (*T*) in (1) at the point *A* (θ, λ), are calculated as derivatives of the respective components of the dipole potential $U = \frac{M}{r^2}\cos\gamma$ (γ is the angle of the dipole axis to the radius vector **r** of *A*).

$$X_c = -\frac{\partial U}{\partial x} = \frac{M}{r^3}\left(2\cos\gamma \frac{\partial r}{\partial x} - r\frac{\partial \cos\gamma}{\partial x}\right);$$

$$Y_c = -\frac{\partial U}{\partial y} = \frac{M}{r^3}\left(2\cos\gamma \frac{\partial r}{\partial y} - r\frac{\partial \cos\gamma}{\partial y}\right);$$

$$Z_c = -\frac{\partial U}{\partial z} = \frac{M}{r^3}\left(2\cos\gamma \frac{\partial r}{\partial z} - r\frac{\partial \cos\gamma}{\partial z}\right).$$

The latter equations include the derivatives along $\cos\gamma = \frac{r^2 + d^2 - a^2}{2rd}$ (*r* and *d* are the lengths of the radius vectors of *A* and of the dipole center relative to the Earth's center, and *a* is the length of the radius vector of *A* relative to the north axial pole), which are given by

$$\frac{\partial \cos\gamma}{\partial x} = K_r \frac{\partial r}{\partial x} + K_a \frac{\partial a}{\partial x};$$

$$\frac{\partial \cos\gamma}{\partial y} = K_r \frac{\partial r}{\partial y} + K_a \frac{\partial a}{\partial y};$$

$$\frac{\partial \cos\gamma}{\partial z} = K_r \frac{\partial r}{\partial z} + K_a \frac{\partial a}{\partial z},$$

$$K_r = \frac{r^2 - d^2 + a^2}{2r^2 d};$$

where

$$K_a = -\frac{a}{rd}.$$

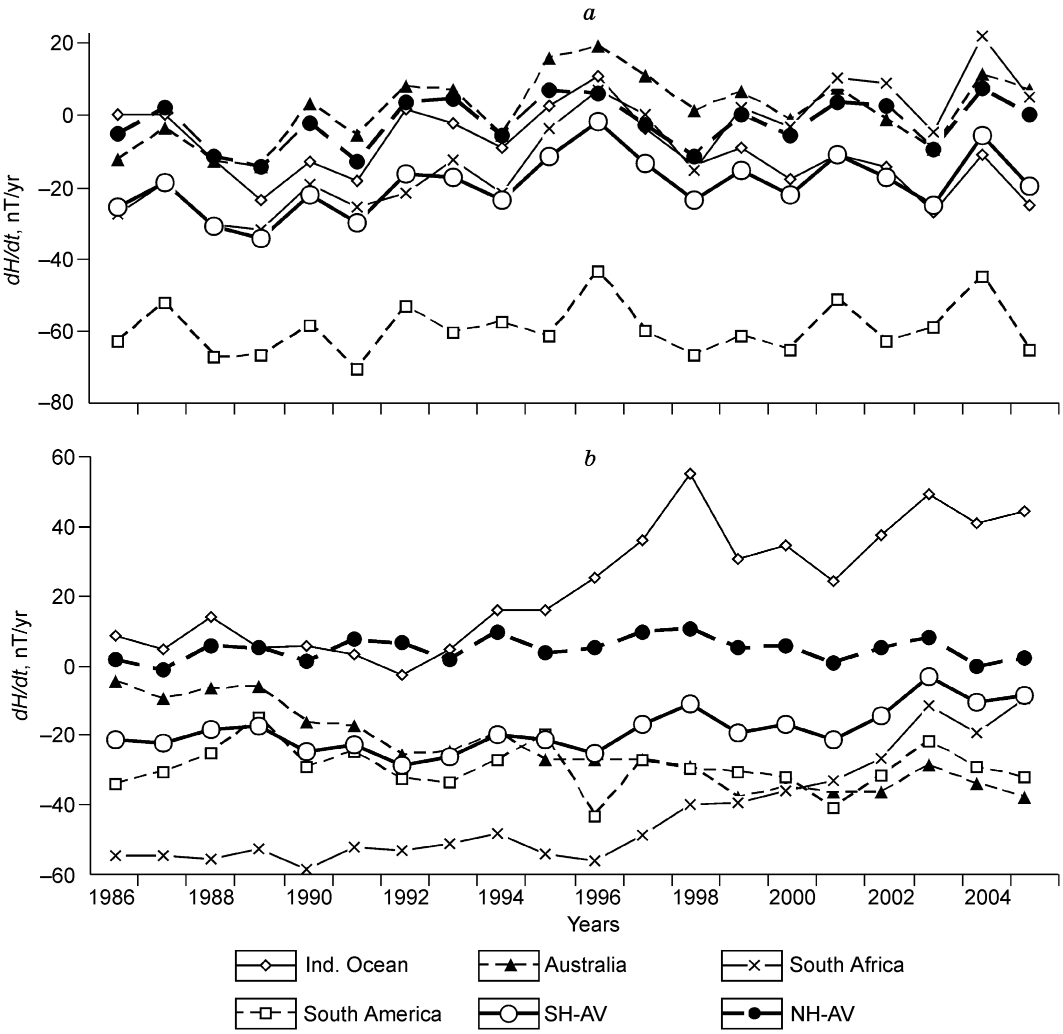

Fig. 5. Variations of H (*a*) and Z (*b*) averaged over southern hemisphere.

The components of the ED field are calculated from the user-specified coordinates of the dipole center and the north ED axial pole.

Table 1 lists the ED parameters: the ED relative distance from the Earth's center r_d, the colatitude θ_d and the longitude λ_d of the dipole center and the colatitude θ_p and the longitude λ_p of the north axial pole estimated using the Excel optimization code by fitting the model dipole fields with varied parameters to IGRF models. The final column in Table 1 shows rms difference between the components of the optimal dipole model and the respective IGRF components.

At the first step we selected the ED parameters that, when changing, would provide fit to the observed phases and amplitudes of the short-period SV peaks. See Table 2 for the phases of the fluctuations and the H and Z amplitudes in the two hemispheres (H_N and H_S, Z_N and Z_S) associated with changes in each parameter allowed to vary.

The observed and computed amplitudes and phases showed no agreement when we changed the dipole center coordinates and the axial pole latitude but fitted well in the case of varied north axial pole longitudes (λ_p), which must be a main factor but not necessarily the only one.

At the next step, each ED parameter was allowed to vary while the others remained fixed (according to the values of 1995 at the locations of HAD and EYR). As we found out, the SV periodicity could be formally fitted to changes of any ED parameter, but the result had to satisfy the condition that the peaks of the tried ED parameter had the same phase in the northern and southern hemispheres. However, the dipole center coordinates were antiphased, and the north axial pole colatitude (θ_p) showed a phase shift and a large amplitude difference (an order of magnitude higher for the northern hemisphere than for the southern one).

It is important to see how the changes in the IGRF ED parameters show up in the H and Z components of the SV field. For this we calculated the geomagnetic components at every five years in 1985 through 2005 using data from www.ngdc.noaa.gov/seg/geomag/jsp/struts/calcPointIGRF and additionally applied fourth-degree polynomial interpolation (Fig. 8).

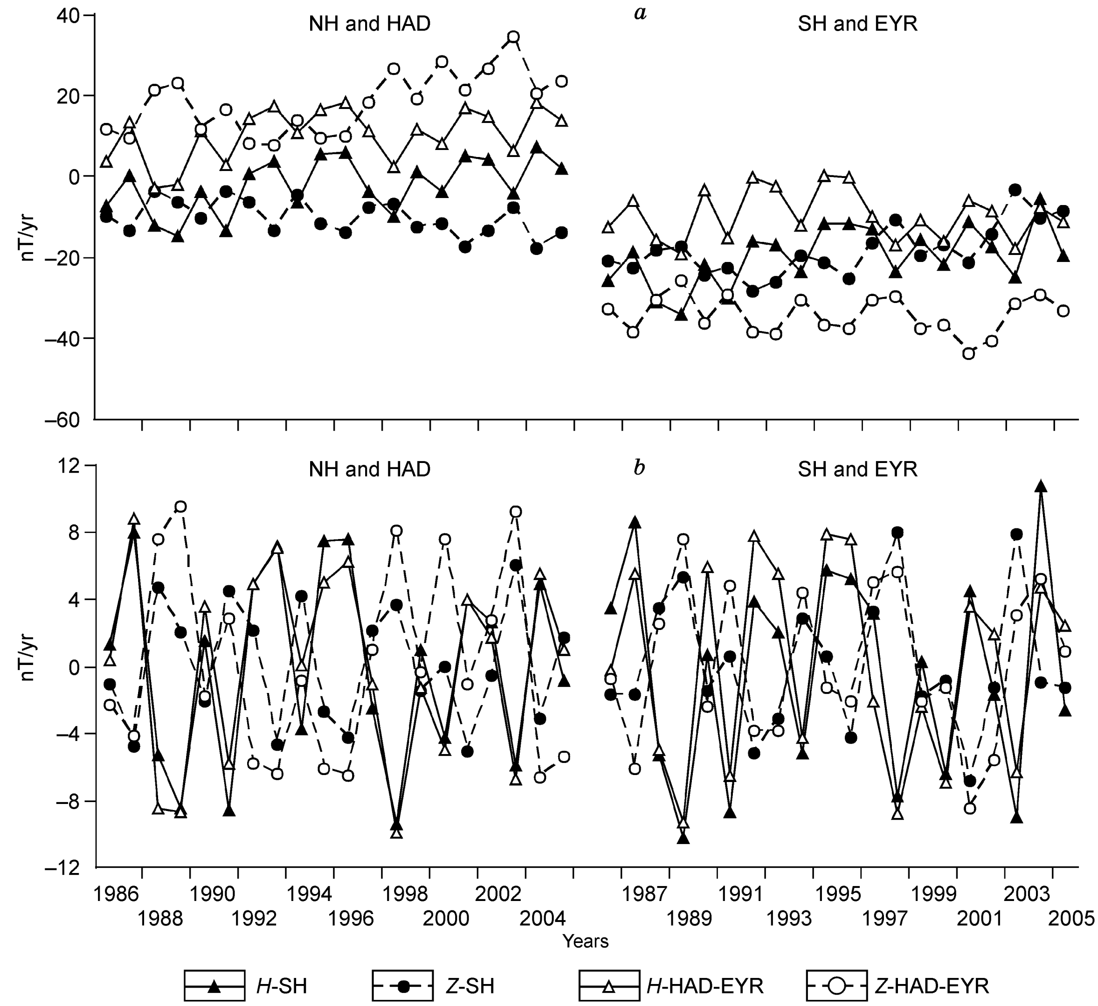

Fig. 6. (*a*) $\Delta H/\Delta t$ and $\Delta Z/\Delta t$ plots; (*b*) same plots with removed regional trends. HAD, EVR are observatories.

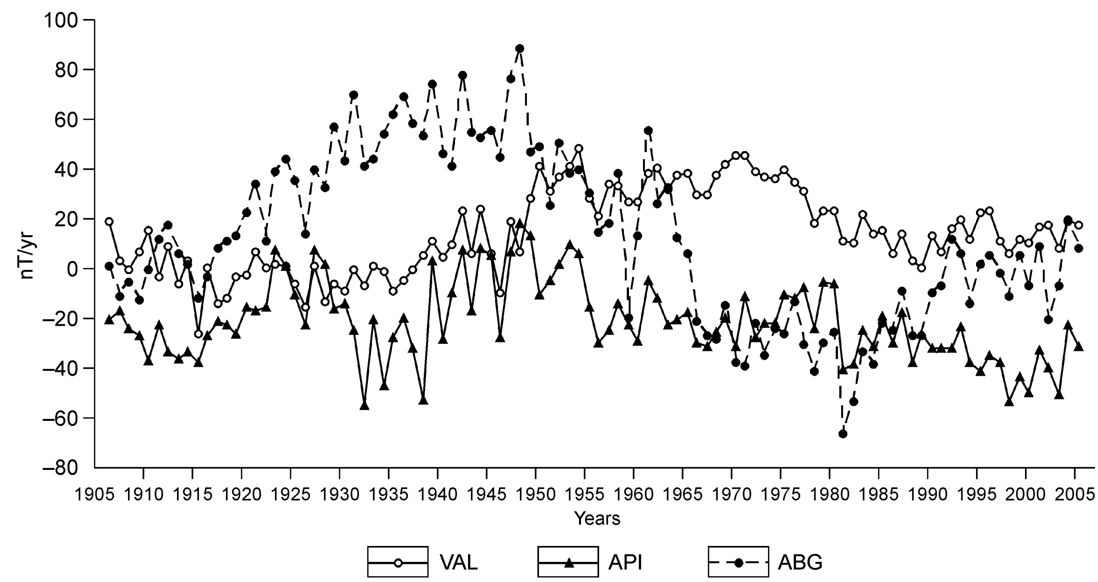

Fig. 7. Variations of *H*, from long series of observatory data. VAL, API, ABG are observatories.

Table 1

Model	Parameter					rms
	r_d	θ_d	λ_d	θ_P	λ_P	
IGRF-1985	0.0920	80.078	144.277	7.192	–82.866	5471
IGRF-1990	0.0941	79.928	143.298	6.923	–83.418	5520
IGRF-1995	0.0963	79.712	142.219	6.627	–84.035	5575
IGRF-2000	0.0985	79.523	140.783	6.257	–84.455	5619
IGRF-2005	0.0993	79.385	140.190	6.124	–84.569	5632

Table 2

Component	Observed data	Varied model parameters				
		r_d	θ_d	λ_d	θ_P	λ_P
H and Z — NH	AP; $H \sim Z$	AP; $> Z$	AP; $H < Z$	AP; $H > Z$	AP; $H > Z$	AP; $H \sim Z$
H and Z — SH	AP; $H \sim Z$	AP; $H \sim Z$	AP; $H > Z$	AP; $H \sim Z$	AP; $H \sim Z$	AP; $H \sim Z$
H — NH and SH	P; $H_N \sim H_S$	AP; $H_N < H_S$	AP; $H_N < H_S$	AP; $H_N < H_S$	AP; $H_N < H_S$	P; $H_N \sim H_S$
Z — NH and SH	P; $Z_N \sim Z_S$	AP; $Z_N < Z_S$	AP; $Z_N > Z_S$	AP; $Z_N < Z_S$	AP; $Z_N < Z_S$	P; $Z_N \sim Z_S$

Note. AP — antiphase, P — in phase, ~ — proximal amplitudes, < or > are notably different variation amplitudes (2–5 times).

The IGRF-derived SV plots are smooth, with dH/dt and dZ/dt antiphased as in observatory data which bear the 2–4 year periodicity, but without this periodicity. This result is consistent with the inference that IGRF models (and other similar models) miss many essential features of geomagnetic secular variation evident in observatory data (Barraclough, 1985; Ladynin et al., 2006a; Lowes, 2003).

The north axial pole coordinates (longitude or colatitude and longitude) were allowed to vary at other ED parameters being fixed according to 1995 observatory data (middle of the 1985–2005 interval) at the locations of HAD and EYR, for each or both hemispheres or for observatories. Note that the accuracy was better in the latter case in all models, because multiple averaging over large areas influenced the dZ/dt values due to the Asian trends.

As we expected, good results were obtained for the north axial pole longitude (Fig. 9). The estimates in Fig. 9 correspond to dH/dt and dZ/dt averaged over the northern and southern hemispheres (NH and SH), (*a*) coupled (NH + SH) at equal pole longitudes in the two hemispheres, and (*b*) separately for each hemisphere. Similar results were obtained from HAD and EYR data (not reported here).

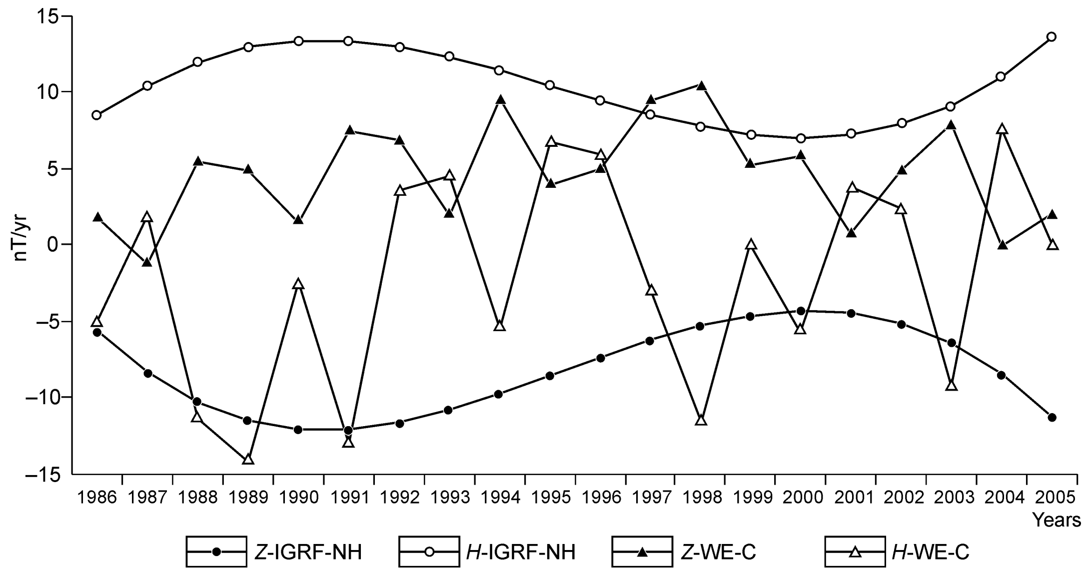

Fig. 8. Variations of *H* and *Z*, estimated from changes in ED parameters in IGRF models compared to those estimated from observatory data of central West Europe.

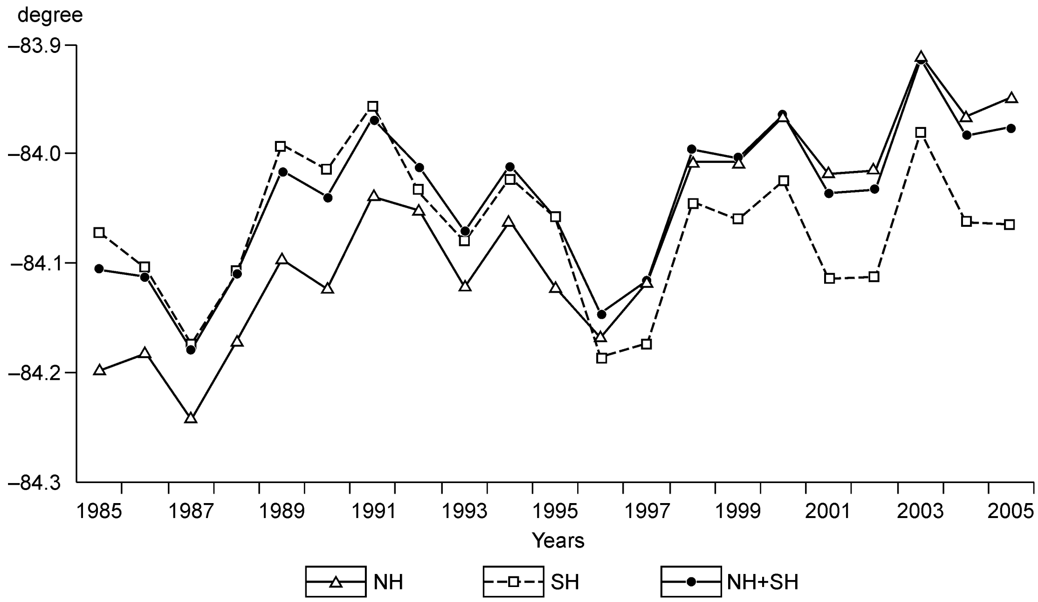

Fig. 9. Variations of north ED longitude according to SV after data of NH, SH, and NH + SH.

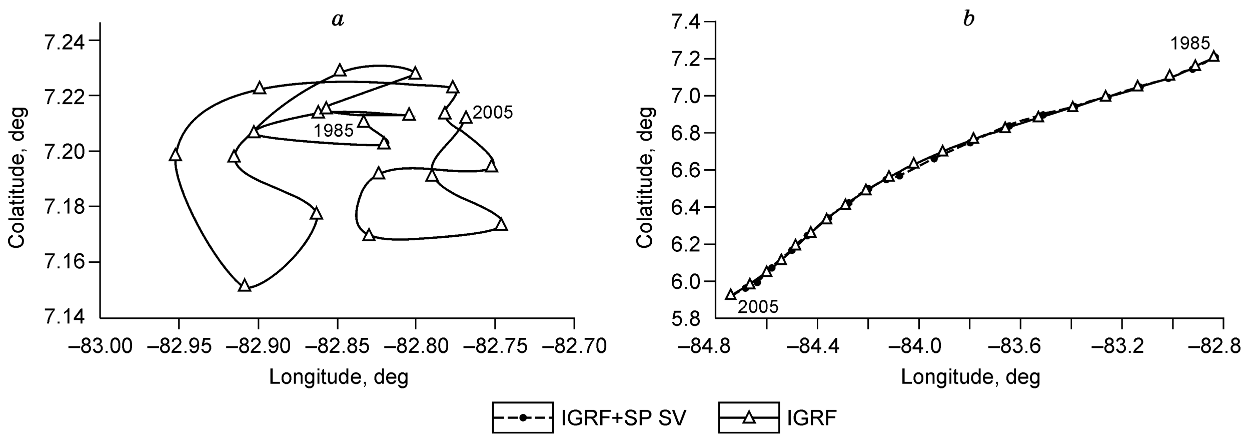

Fig. 10. Positions of north ED axial pole. *a* — estimated from *H* and *Z* variations (regional trends removed in form of fourth-degree polynomial); *b* — estimated from IGRF models (solid line), with superposed plot (dashed line) including data of panel (*a*): coupled IGRF + short-period SV.

Variations in the pole colatitude were within 0.08° and the difference between the respective values in different models (cases *a* and *b*) was less than 0.05°, while the same variations of longitude were two or three times larger.

The main result, the drift of the north axial pole inferred from the 2–4 year SV periodicity, as an average for the two hemispheres, is shown in Fig. 10 *a*. The panel (*b*) of the same figure shows the IGRF pole positions during the interval 1985 to 2005 superposed by a plot (dashed line) including data of the panel (*a*).

These plots may explain the absence of the short-wavelength SV periodicity from the IGRF analytical models: The deviations are too small to be resolved at the existing accuracy of the latter. IGRF models are mostly based on total intensity (T) measurements, with some previous field model taken for the initial approximation T_0; the spherical harmonic coefficients are corrected until the model values $T = T_0 + \delta T$ coincide with observed data. The field variation δT is introduced using the linear differential equation

$$\delta T = \delta X \frac{X_0}{T_0} + \delta Y \frac{Y_0}{T_0} + \delta Z \frac{Z_0}{T_0}, \quad (2)$$

where $\delta \mathbf{T}$ is found as a sum of projections of the vector components onto the $\mathbf{T}_0$ direction; $\mathbf{T}_0$ being directed along the dipole field, the non-dipole components are actually neglected. The exact changes ΔT are given by

$$\Delta T = \sqrt{(X_0 + \delta X)^2 + (Y_0 + \delta Y)^2 + (Z_0 + \delta Z)^2} - T_0. \quad (3)$$

The deviation of δT from the exact ΔT is small as the former is a linear approximation of the latter. Secular variations of the $\mathbf{T}$ vector are expressed via the variations of the components as

$$T_V = \sqrt{\delta X^2 + \delta Y^2 + \delta Z^2}. \quad (4)$$

If the field changes linearly and the direction remains invariable (as in the case of scaling), δT and T_V coincide. The stability of the D and I components at each point means that the dipole does not change its direction. These ideas are consistent with comparison of satellite (IGRF) and observatory SV estimates (Ladynin et al., 2006a) which shows that the IGRF secular variation plots agree with the measured observatory data in mean amplitudes but disagree in the pattern of variations.

The position of the north axial pole changed for 0.15–0.19° according to the quasi-periodic fluctuations, whereas the total change according to the IGRF 1985–2005 models is an order of magnitude greater.

Discussion

The geomagnetic dipole is a mathematical abstraction, its physics being associated with ring current in the liquid core. The eccentric dipole model implies a complex current system, with its symmetry axis (dipole axis) tilted toward the Earth's spin axis and set off the center toward the western Pacific. Furthermore, the dipole is drifting northward relative to the geographic equatorial plane, and the drift increases with time (Fraser-Smith, 1987).

In the IGRF 1900–2005 models, the field shows a 0.065% mean annual decrease in the first harmonic coefficients $(g_{10}^2 + g_{11}^2 + h_{11}^2)^{1/2}$ and a 0.28% mean annual increase in the higher-order terms (2–10). There are also other markers of the dipole field decline (all data for 50 years), namely (a) increasing rms errors in the ED approximation of the geomagnetic field (9.1%), (b) greater rms values of ED harmonic coefficients from $m = 2$ to 5; (*c*) an almost double increase of the rms approximation of the ED field by a series with $m = 5$.

The quasi-periodic fluctuations of the dipole field record changes in the respective current systems. These changes may be part of a mechanism which gradually destroys the dipole field before its reversal. A similar short-wavelength periodicity superposed on long-period cycles was reported for geodynamic processes such as upper mantle convection and formation of lower mantle plumes (Dobretsov et al., 2001).

The instability of the dipole field is known also in paleomagnitology (Braginskii, 1978; Khramov et al., 1982). The short-period fluctuations of the dipole field are important in theoretical modeling of the geomagnetic field generated by current systems in the liquid core.

Long-period geomagnetic secular variations are not related with the dipole field but are rather associated with convective flows on the core surface (Parkinson, 1983; Warding, 2005, etc.). These variations have geodynamic implications as the ascending core surface flows are suggested to be responsible for thermal or thermochemical plumes rising from the lower mantle D″ layer which are currently assumed to be the original cause of global geodynamic processes (Dobretsov et al., 2001).

Thorough investigation into the reported periodicity will allow us to remove it from decadal or longer-period geomagnetic secular variations which appear in the form of jerks (Currie, 1976; Courtillot and Le Mouel, 1984; Huy et al., 1998; Kerridge and Barraclough, 1985). Inasmuch as the long-period SV are related to core surface flows, one may expect to update the space-time structure of these flows and the respective position of the plume sources.

Conclusions

We discovered a 2–4 year periodicity in geomagnetic secular variation. The periodicity being globally uniform in various regions of the world, on all continents, and in both hemispheres, it was attributed to oscillations of the dipole axis. We estimated the drift of the north axial pole from dH/dt and dZ/dt variations to be 0.15–0.2° for 20 years, which is an order of magnitude smaller than that estimated from IGRF models.

The short-period variations of the geomagnetic field may result from instability of the core surface convective flow responsible for the generation of the dipole field, the largest constituent of the main field.

References

Backus, G.E., 1974. Non-uniqueness of the external geomagnetic field determined by surface intensity measurements. Geophys. Res. 75, 6337–6341.

Barraclough, D.R., 1976. Spherical harmonic analysis of the geomagnetic secular variation. A review of methods. Phys. Earth Planet. Inter. 12, 365–387.

Barraclough, D.R., 1985. A comparison of satellite and observatory estimates of geomagnetic secular variation. J. Geophys. Res. 90 (B3), 2523–2526.

Ben'kova, N.P., Golovkov, V.P., Cherevko, T.N., 1979. Estimating the westerly drift of the geomagnetic field. Geomagnetizm i Aeronomiya 19 (3), 579–581.

Ben'kova, N.P., Pushkov, A.N., 1978. The geomagnetic field, in: Ben'kova, N.P. (Ed.), Results in Science and Technology. Geomagnetism and Upper Atmosphere [in Russian]. Book 5, pp. 5–95.

Braginskii, C.I., 1978. Geomagnetic dynamo. Izv. AN SSSR, Ser. Fizika Zemli, No. 9, 74–90.

Courtillot, V., Le Mouel, J.-L., 1984. Geomagnetic secular variation impulses. Nature 311, 709–716.

Currie, R.G., 1976. Long-period magnetic activity — 2 to 100 years. Astrophys. Space Sci. 9, 251–254.

Dipole Approximations of the Geomagnetic Field, 2003. www.spenvis.oma.be.

Dobretsov, N.L., Kirdyashkin, A.G., Kirdyashkin, A.A., 2001. Deep Geodynamics [in Russian], 2nd edition. Izd. SO RAN, Filial "Geo", Novosibirsk.

Dolginov, Sh.Sh., Ivchenko, M.P., Orlov, V.P., Pushkov, A.N., Tyurmina, L.O., Cherevko, T.N., 1972. Secular geomagnetic field variation of the epoch 1965–1970, according to observatory and satellite data. Geomagnetizm i Aeronomiya 12 (3), 503–512.

Fadel, Kh.M., Semenov, A.I., Shefov, N.N., Sukhodoev, V.A., Martsveladze, N.M., 2002. Quasi-biannual variations in mesopause temperature, lower thermosphere, and solar activity. Geomagnetizm i Aeronomiya 27 (2), 203–207.

Fraser-Smith, A.C., 1987. Centered and eccentric geomagnetic dipoles and their poles, 1600–1985. Rev. Geophys. 25 (1), 1–16.

Gauss, K.F., 1839. Allgemeine Theorie des Erdmagnetismus, in: Gauss, K.F., Weber, W. (Eds.), Resultate aus den Beobachtungen des Magnetischen Vereins im Jahre 1838. Leipzig, pp. 1–57.

Huy, M., Alexandrescu, M., Le Mouel, J.-L., 1998. On the characteristics of successive jerks. Earth Planets Space 50, 723–732.

Ivanov-Kholodnyi, G.C., Mogilevskii, E.I., Chertoprud, V.E., 2002. Solar and ionospheric quasi-biannual variations. Geomagnetizm i Aeronomiya 27 (2), 199–202.

Kalinin, Yu.D., 1984. Geomagnetic Secular Variation [in Russian]. Nauka, Novosibirsk.

Kerridge, D. J., Barraclough, D. R., 1985. Evidence for geomagnetic jerks from 1931 to 1971. Phys. Earth Planet. Inter. 39, 228–236.

Langel, R.A., 1987. The main field, in: Jacobs, J.A. (Ed.), Geomagnetism. Academic Press, London, Book 1, pp. 249–492.

Khramov, A.N., Goncharov, G.I., Komissarova, R.A., Pisarevskii, S.A., Pogorskaya, I.A., Rzhevskii, Yu.S., Rodionov, V.P., Slautsitis, I.P., 1982. Paleomagnitology [in Russian]. Nedra, Leningrad.

Ladynin, A.V., 2008. Potential Geophysical Fields: Geological Applications. A Manual [in Russian]. Novosibirsk. Gos. Univ., Novosibirsk.

Ladynin, A.V., Popova, A.A., Semakov, N.N., 2006a. Geomagnetic secular variations: satellite against observatory data. Russian Geology and Geophysics (Geologiya i Geofizika) 47 (2), 278–291 (284–298).

Ladynin, A.V., Popova, A.A., Khomutov, S.Yu., 2006b. Short-period geomagnetic secular variations, from observatory data, in: 170 Years of Observatory Measurements in the Urals: History and State of the Art. Intern. Workshop, Ekaterinburg, 17–23 July 2006. Ekaterinburg.

Lowes, F.J., 2000. An estimate of the errors of the IGRF/DGRF fields 1945–2000. Earth Planets Space 52 (12), 1207–1211.

Lowes, F.J., 2003. The International Geomagnetic Reference Field: A "Health" Warning. IAGA Division V-MOD. Geomagnetic Field Modeling: IGRF proper use.

Observatory List by IAGA Code. www.wdc.bgs.ac.uk/catalog/master.html

Parkinson, W.D., 1983. Introduction to Geomagnetism. Scottish Academy Press, Edinburgh-London.

Pushkov, A. N., 1972. On possibility to estimate geomagnetic secular variation from the total field vector distribution. Geomagnetizm i Aeronomiya 12 (3), 519–523.

Wardinski, I., 2005. Core surface flow models from decadal and subdecadal secular variation of the main geomagnetic field. GFZ, Potsdam.

www.bgs.ac.uk/images/charts/jpg

www.geomag.bgs.ac.uk/cgi-bin/means

www.ngdc.noaa.gov/seg/geomag/jsp/struts/calcPointIGRF

Yanovskii, B.M., 1978. Geomagnetism [in Russian], Izd. Leningr. Univ., Leningrad.

Editorial responsibility: M.I. Epov